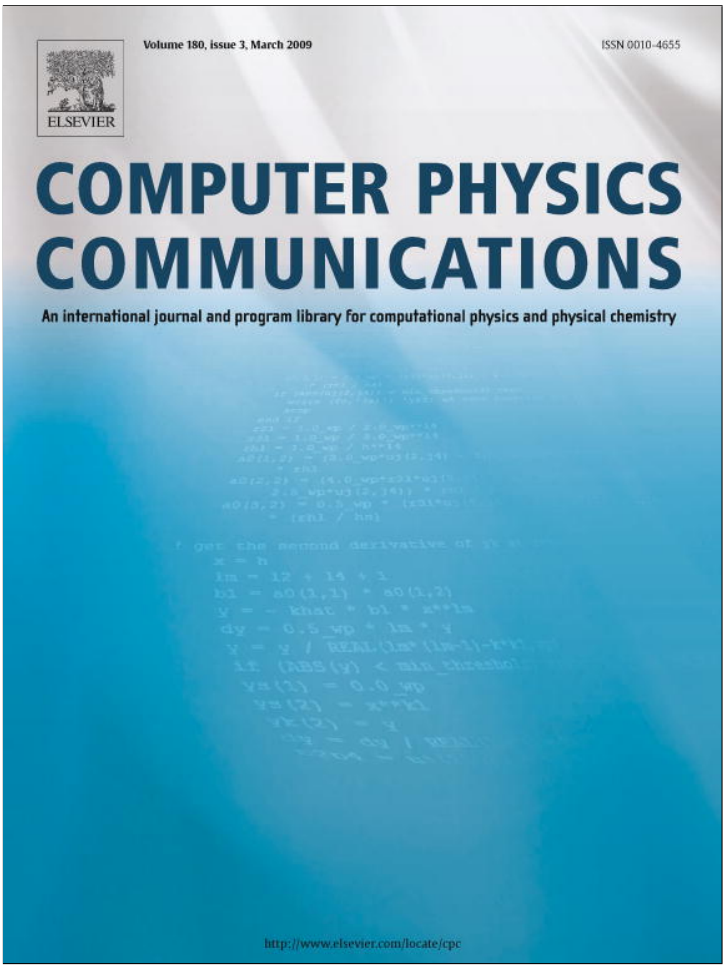

Computer Physics Communications 180 (2009) 401–417

Contents lists available at ScienceDirect

Computer Physics Communications

www.elsevier.com/locate/cpc

PHANTOM: A Monte Carlo event generator for six parton final states at high energy colliders ☆

Alessandro Ballestrero [a], Aissa Belhouari [c], Giuseppe Bevilacqua [a,b], Vladimir Kashkan [a,b], Ezio Maina [a,b,*]

[a] INFN, Sezione di Torino, Italy
[b] Dipartimento di Fisica Teorica, Università di Torino, Italy
[c] The Abdus Salam International Center for Theoretical Physics, Trieste, Italy

ARTICLE INFO

Article history:
Received 10 June 2008
Received in revised form 28 August 2008
Accepted 7 October 2008
Available online 11 October 2008

PACS:
12.15.-y
11.15.Ex

Keywords:
Six fermions
Electroweak symmetry breaking
Higgs
Top
LHC
Linear collider

ABSTRACT

PHANTOM is a tree level Monte Carlo for six parton final states at proton–proton, proton–antiproton and electron–positron colliders at $\mathcal{O}(\alpha_{EM}^6)$ and $\mathcal{O}(\alpha_{EM}^4\alpha_S^2)$ including possible interferences between the two sets of diagrams. This comprehends all purely electroweak contributions as well as all contributions with one virtual or two external gluons. It can generate unweighted events for any set of processes and it is interfaced to parton shower and hadronization packages via the latest Les Houches Accord protocol. It can be used to analyze the physics of boson–boson scattering, Higgs boson production in boson–boson fusion, $t\bar{t}$ and three boson production.

Program summary

Program title: PHANTOM (V. 1.0)
Catalogue identifier: AECE_v1_0
Program summary URL: http://cpc.cs.qub.ac.uk/summaries/AECE_v1_0.html
Program obtainable from: CPC Program Library, Queen's University, Belfast, N. Ireland
Licensing provisions: Standard CPC licence, http://cpc.cs.qub.ac.uk/licence/licence.html
No. of lines in distributed program, including test data, etc.: 175 787
No. of bytes in distributed program, including test data, etc.: 965 898
Distribution format: tar.gz
Programming language: Fortran 77
Computer: Any with a UNIX, LINUX compatible Fortran compiler
Operating system: UNIX, LINUX
RAM: 500 MB
Classification: 11.1
External routines: LHAPDF (Les Houches Accord PDF Interface, http://projects.hepforge.org/lhapdf/), CIRCE (beamstrahlung for e^+e^- ILC collider).
Nature of problem: Six fermion final state processes have become important with the increase of collider energies and are essential for the study of top, Higgs and electroweak symmetry breaking physics at high energy colliders. Since thousands of Feynman diagrams contribute in a single process and events corresponding to hundreds of different final states need to be generated, a fast and stable calculation is needed.
Solution method: PHANTOM is a tree level Monte Carlo for six parton final states at proton–proton, proton–antiproton and electron–positron colliders. It computes all amplitudes at $O(\alpha_{EM}^6)$ and $O(\alpha_{EM}^4\alpha_s^2)$ including possible interferences between the two sets of diagrams. The matrix elements are computed with the helicity formalism implemented in the program PHACT [1]. The integration makes use of an iterative–adaptive multichannel method which, relying on adaptivity, allows the use of only a few channels per process. Unweighted event generation can be performed for any set of processes and it is interfaced to parton shower and hadronization packages via the latest Les Houches Accord protocol.
Restrictions: All Feynman diagrams are computed al LO.

☆ This paper and its associated computer program are available via the Computer Physics Communications homepage on ScienceDirect (http://www.sciencedirect.com/science/journal/00104655).

* Corresponding author.
E-mail address: maina@to.infn.it (E. Maina).

0010-4655/$ – see front matter
doi:10.1016/j.cpc.2008.10.005

Unusual features: Phantom is written in Fortran 77 but it makes use of structures. The g77 compiler cannot compile it as it does not recognize the structures. The Intel, Portland Group, True64 HP Fortran 77 or Fortran 90 compilers have been tested and can be used.
Running time: A few hours for a cross section integration of one process at per mille accuracy. One hour for one thousand unweighted events.
References:
[1] A. Ballestrero, E. Maina, Phys. Lett. B 350 (1995) 225, hep-ph/9403244;
A. Ballestrero, PHACT 1.0, *Program for helicity amplitudes Calculations with Tau matrices*, hep-ph/9911318, in: B.B. Levchenko, V.I. Savrin (Eds.), *Proceedings of the 14th International Workshop on High Energy Physics and Quantum Field Theory (QFTHEP 99)*, SINP MSU, Moscow, p. 303.

1. Introduction

Monte Carlo event generators are essential tools for the comparison of theory and experiment in High Energy Physics. In this paper we present PHANTOM a new event generator which is capable of simulating any set of reactions with six partons in the final state at pp, $p\bar{p}$ and e^+e^- colliders at $\mathcal{O}(\alpha_{EM}^6)$ and $\mathcal{O}(\alpha_{EM}^4\alpha_S^2)$ including possible interferences between the two sets of diagrams. This includes all purely electroweak contributions as well as all contributions with one virtual or two external gluons. The relevance of six fermion final states both at the LHC and the ILC is well known and will be further discussed in Section 2. The signal of processes like Higgs boson production in vector boson fusion with a Higgs decaying in two bosons, boson–boson scattering and 3-vector boson production are all described by 6 fermion final states at $\mathcal{O}(\alpha_{EM}^6)$. Top–antitop pair production is also described by a six fermion final state and its signal is at $\mathcal{O}(\alpha_{EM}^6)$ for the ILC but at hadron colliders the main contribution comes from $\mathcal{O}(\alpha_{EM}^4\alpha_S^2)$.

As far as the irreducible backgrounds to the above mentioned signal is concerned, $\mathcal{O}(\alpha_{EM}^4\alpha_S^2)$ reactions encompass the full lowest order QCD background for six-parton studies of final states with four leptons at hadron colliders. An example is VV fusion with fully leptonic decays of the intermediate vector bosons. On the contrary, semileptonic channels get additional contributions from $\mathcal{O}(\alpha_{EM}^2\alpha_S^4)$ processes which are responsible for the V + 4 *jets* background. The latter must be included as well in a complete analysis and can be covered by other Monte Carlo event generators, such as AlpGen [1] or MadEvent [2]. It should be noticed nevertheless that these contributions have quite different kinematical features with respect to the scattering signature, therefore they are expected to be suppressed by means of appropriate selection cuts.

At e^+e^- colliders there is no QCD background for six and four lepton final states and $\mathcal{O}(\alpha_{EM}^4\alpha_S^2)$ reactions describe completely the QCD background to final states with two leptons. Only for fully hadronic final states the set of reactions presently available in PHANTOM needs to be complemented by other generators.

PHANTOM employs exact tree matrix elements. There are issues which cannot be tackled without a complete calculation, like exact spin correlations between the decays of different heavy particles, the effect of the non-resonant background, the relevance of the offshellness of boson decays, the question of interferences between different subamplitudes. Without a full six parton computation it will be impossible to determine the accuracy of approximate estimates. In Ref. [3] the complete calculation for $PP \to 4j\mu\bar{\nu}_\mu$ at $\mathcal{O}(\alpha_{EM}^6)$ has been compared at length with a production times decay approach, showing differences of the order of 10–20% in some important regions of phase space. The reliability of the Equivalent Vector Boson Approximation (EVBA) [4] in the context of vector boson scattering has been critically examined in [5].

PHANTOM is an example of a *dedicated* event generator which describes a predefined set of reactions striving for maximum speed and efficiency. Other recent examples of dedicated programs for LHC physics are Toprex [6], which provides the matrix elements for several reactions related to top production, Alpgen [1] and Gr@ppa [7]. Alpgen can simulate a large number of processes with electroweak bosons and heavy quarks plus jets. When more than one electroweak boson are present in the final state they are considered to be on shell. Gr@ppa provides event generators for V (W or Z) + jets ($\leqslant$4 jets), VV + jets ($\leqslant$2 jets) and QCD multi-jet ($\leqslant$4 jets) processes.

Dedicated generators aimed at future e^+e^- colliders are Lusifer [8], which covers all reactions with six massless fermions in the final state at $\mathcal{O}(\alpha_{EM}^6)$ and $\mathcal{O}(\alpha_{EM}^4\alpha_S^2)$, SIXFAP [9], which covers all reactions with six fermions in the final state at $\mathcal{O}(\alpha_{EM}^6)$ including mass effects, SIXPHACT [10], which was among the first MC to compute six fermion final states but was limited to processes with one final neutrino, eett6f [11], which simulates only processes related to top–antitop production and SIXRAD [12], which deals with all six jet final states at $\mathcal{O}(\alpha_{EM}^2\alpha_S^4)$.

The Monte Carlo's just mentioned show that six fermion physics has been already investigated at the ILC since a long time and they have been used for several phenomenological studies. PHANTOM is the first complete dedicated Monte Carlo which extends this kind of physics to hadron colliders.

The complementary approach is given by *multi-purpose* programs for the automatic generation of any user-specified parton level process. The following codes for multi-parton production are available: Amegic-Sherpa [13], CompHEP [14], Grace [15], Madevent [2], Phegas & Helac [16], O'Mega & Whizard [17]. CompHEP is limited to processes with at most eight external particles but since it computes matrix elements squared instead of helicity matrix elements it is extremely slow when a large number of particles is involved. Grace is a framework for generating single process matrix elements which can be interfaced to integration and event generator modules. The remaining packages, Amegic-Sherpa, Madevent, Phegas & Helac and O'Mega & Whizard are complete event generators which automatically generate the amplitudes, produce the mappings for integration over phase space, compute cross sections and generate unweighted events. While processes with six particles in the final states can be tackled with these generators, see for instance [18], they are at the limit of their practical capabilities when the unweighted generation of several hundreds of this kind of processes is involved, as it is needed for LHC physics.

PHANTOM profits from the experience obtained with PHASE [19] which could only simulate all electroweak processes of the type $PP \to 4q + l\nu_l$ at the LHC. The two codes share a number of key features. The matrix elements are computed with the use of the modular helicity formalism of Refs. [20,21] which is well suited to compute in a fast and compact way parts of diagrams of increasing size, and

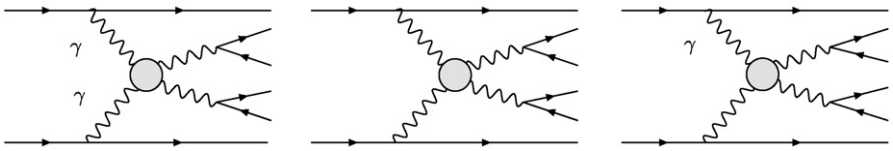

Fig. 1. Vector boson fusion processes.

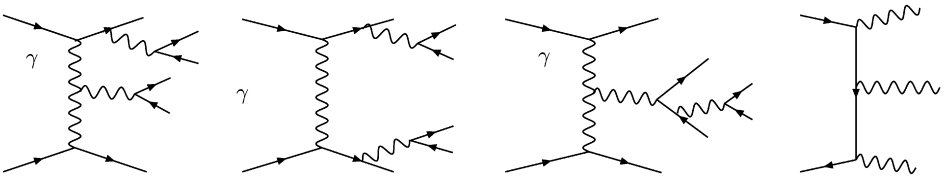

Fig. 2. Non-fusion and non-doubly resonant two vector boson production. Three vector boson production.

recombine them later to obtain the final set. The integration strategy merges the multichannel approach [22] with the adaptivity of VEGAS [23]. This results in generators which adapt to different kinematical cuts and peaks with good efficiency, using only few channels per process. Both codes employ the *one-shot* method developed for WPHACT [24], and used for four-fermion data analyses at LEP2. In this running mode, all processes are simultaneously generated in the correct relative proportion for any set of experimental cuts.

The paper is organized as follows: in Section 2 we examine the physical content of the processes which can be described by PHANTOM. Then Section 3 describes the features of the program, the way amplitudes are calculated, phase spaces are implemented and integration is performed. The following section is dedicated to the modes of operating the program and finally Section 5 reports an example of the phenomenological studies which can be performed using PHANTOM.

2. Physical processes

Processes with six partons in the final state will be central to the physics program at next generation accelerators, the LHC [25,26] and the ILC [27]. They include Higgs boson production in vector boson fusion followed by Higgs decay to WW and ZZ, boson–boson scattering processes, top–antitop pair production, three vector boson production.

The Standard Model (SM) provides the simplest and most economical explanation of Electro-Weak Symmetry Breaking (EWSB) in terms of a single Higgs doublet. The search for the Higgs sector and its investigation will have the highest priority for all LHC experiments [28–30]. Detailed reviews and extensive bibliographies can be found in Refs. [31–33]. In the SM the Higgs is essential to the renormalizability of the theory and is also crucial to ensure that perturbative unitarity bounds are not violated in high energy reactions. In particular, if no Higgs is present in the spectrum, longitudinally polarized vector bosons interact strongly at high energy, violating perturbative unitarity at about one TeV [34]. If, on the contrary, a relatively light Higgs exists then they are weakly coupled at all energies. These processes have been scrutinized since a long time, going from the pioneering works in [35,36], which address boson–boson scattering on a general ground, to the more recent papers in [37,38] focused on the extraction of signals of vector boson scattering at the LHC. In the last few years QCD corrections to boson–boson production via vector boson fusion [39] and to three vector boson production [40] at the LHC have been computed. The size of the corrections depends quite strongly on the particular process under consideration: while in the boson fusion case the corrections are below 10%, for the three boson production case they are in the 70 to 100% range.

Top pair production with its large cross section and large signal to background ratio will play a central role since the early days of data taking at the LHC. The measurement accuracy will quickly be dominated by systematic effects, in particular by b-jet energy scale uncertainties, while statistical errors will be negligible. The wealth of available channels will provide feedback on the detector performance and assist in detector calibration [25,26]. A total error on the top mass of about 2 GeV is expected to be feasible. Exploiting the high statistics it will be possible to search for new physics signatures in top production and decay. Spin correlations will be measured to a precision of a few percent. Finally, a good understanding of top physics will be essential since top production will be a major source of background for all investigations of processes involving high p_T W's, like boson–boson scattering and many new physics searches.

PHANTOM is intended in particular for studies of Higgs, boson–boson scattering and top physics in six fermion final states. It can compute all processes of this kind and does not make use of any production times decay (narrow width) or equivalent vector boson approximation. This implies that every single diagram contributing to a definite final state is included and not only the resonant ones. So for instance if one studies a vector boson fusion process not only the diagrams reported in Fig. 1 will be considered but also, when appropriate, all other diagrams of the types described in Figs. 2–4. In the same way when studying top–antitop production not only the first two diagrams on the left of Fig. 4 will be considered but all the others schematically described in the rest of Fig. 4 and also in the other three figures. Moreover all diagrams which do not have two resonant bosons in the final state contribute as well. We have already discussed in some particular cases [3,5,10] the differences between a complete calculation and an approximated one. These depend on the particular physical study at hand and on the applied cuts. But a complete calculation is in any case an important tool to quantify the possible discrepancies.

Let us explain with one example which are the processes to be included in a practical case. Suppose one wants to study a Higgs produced in boson–boson fusion decaying to two W's with one of the W's decaying leptonically. In such a case one will experimentally search for a signal of four jets plus a lepton and missing transverse momentum. The corresponding physical processes that will have to be generated with PHANTOM are all those with a lepton and a neutrino and 4 quarks in the final state at $\mathcal{O}(\alpha_{EM}^6) + \mathcal{O}(\alpha_{EM}^4 \alpha_S^2)$ as well as those with one or two outgoing gluons and three or two quarks in addition to the leptons. The number of these processes amounts to a few hundreds. The unweighted generation of all of them will be performed simultaneously with PHANTOM.

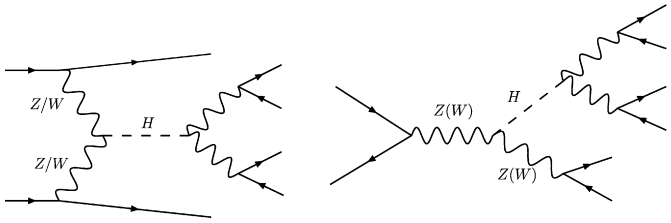

Fig. 3. Higgs boson production via vector boson fusion and Higgsstrahlung.

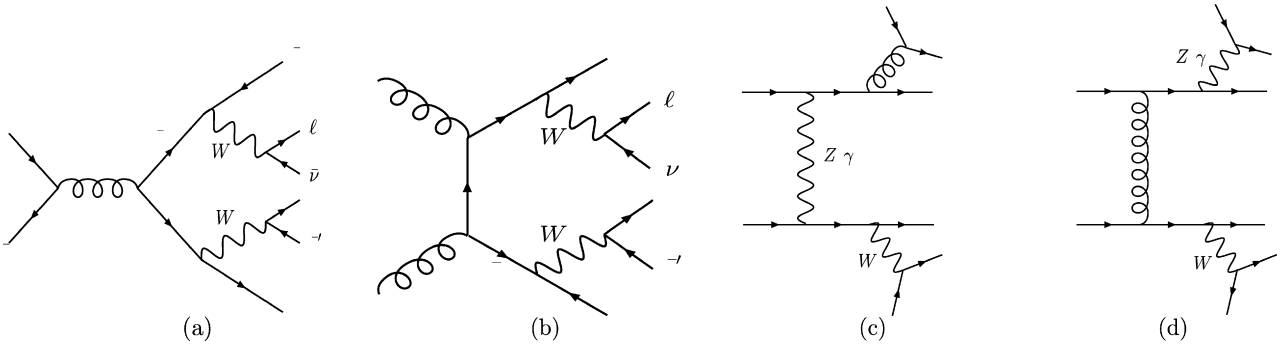

Fig. 4. Examples of contributions to the QCD irreducible background: $t\bar{t}$ production (a, b) and VV + 2 jets (c, d).

Analogous considerations hold of course for top–antitop or boson–boson scattering studies. One cannot separate the different physical processes just considering the final states, and the strategy is that of a full calculation. With a complete sample one will thereafter evidentiate the physics of interest with appropriate cuts.

3. Program description

We give in this section a description of the main features of the PHANTOM Monte Carlo. The routine list and an example of input file for running the program are presented in Appendices A and B, respectively. A User Guide can be found in the PHANTOM distribution, with more details on how to run the program and how to prepare the input files.

3.1. General features

As already said, PHANTOM can generate unweighted event samples for any set of reactions with six partons in the final state at pp, $p\bar{p}$ and e^+e^- colliders at $\mathcal{O}(\alpha_{EM}^6)$ and $\mathcal{O}(\alpha_{EM}^4\alpha_S^2)$. Possible interferences between the two sets of diagrams can be taken into account. Alternatively, the user can simulate purely electroweak and $\mathcal{O}(\alpha_{EM}^4\alpha_S^2)$ processes separately. All finite width effects are taken into account as well as all correlations between the decay of any unstable particle which appear in intermediate states. In most cases, with the notable exception of $t\bar{t}$ production, the purely electroweak contribution contains the physical processes we wish to investigate, while the contributions with one virtual or two external gluons represent a background. In particular $\mathcal{O}(\alpha_{EM}^4\alpha_S^2)$ processes completely describe VVjj productions at hadron colliders and V4j at e^+e^- machines.

The program proceeds in two steps which are performed separately. In the first phase each of the reactions which need to appear in the final event sample is integrated over and the corresponding cross section is calculated. At the same time the density of points in the unit cube employed for the sampling is recursively modified in order to match the actual behavior of the integrand and the integrand maximum is searched for. The information gathered in this step is stored in the form of an integration grid. In the final stage all the grids and maxima are used to produce the unweighted event sample. The separation between the two phases allows for additional flexibility: the grids produced with a specified set of acceptance cuts can be used to produce event samples with any set of more restrictive selection cuts or for a smaller number of reactions without repeating the integration step. Additional processes can easily be introduced.

The number of reactions which contribute to a given final state, say for instance $4jl\nu$, can be very large, particularly at hadron colliders. In our approach it is crucial to keep the number of reactions for which the individual cross section needs to be computed to a minimum. By making use of symmetries, the task of computing all relevant processes can be substantially simplified. Indeed all reactions which differ by charge conjugation and by the symmetry between the first and second quark families can be described by the same matrix element, provided one take a diagonal CKM matrix and ignores the light quark masses. This extends to processes which are related by a permutation of the lepton families. At most they differ by the PDF's convolution and possibly by a parity transformation, which can be accounted for automatically. In the integration step the user can sum over all processes which are related by charge and family symmetries setting the flag `i_ccfam`.

3.2. Amplitudes

The matrix elements are computed with the helicity formalism of Ref. [20] and the semi-automatic method described in Ref. [21]. In our experience the resulting amplitudes are much faster than those obtained by completely automatic procedures. Even though we have not made a detailed comparison with all programs and for all kind of amplitudes, we happened for instance to find differences in CPU time of one order of magnitude or more with Madgraph, in agreement with the statements in Ref. [39].

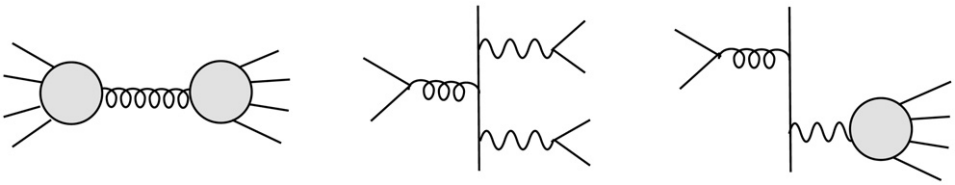

Fig. 5. Gluon exchange diagrams.

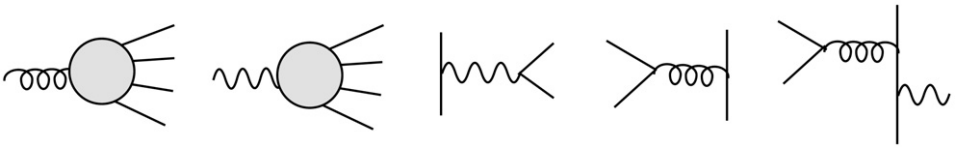

Fig. 6. Gluon exchange subdiagrams.

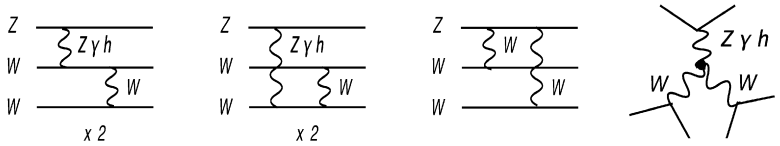

Fig. 7. Electroweak configurations of 2g2WZ.

In our calculation we first of all take advantage of the well known fact that all processes which share the same total particle content, with all partons taken to be outgoing, can be described by a single master amplitude.

The calculation can be further simplified examining more closely the full set of Feynman diagrams. Since we assume a diagonal CKM matrix, the fermion–antifermion pair appearing at the end of a given fermion line either are of the same flavor, if only neutral vector insertion or an even number of W insertions take place along the line, or reconstruct an isospin doublet if an odd number of W insertions takes place. Therefore, limiting ourselves to reactions in which all external particles are fermions it becomes quickly apparent that in some processes, fermions can be paired only into neutral couples (we indicate them as 4Z), e.g., $u\bar{c} \to u\bar{c}\mu\bar{\mu}e\bar{e}$, while in others only charged couples can be formed (4W), e.g., $u\bar{d} \to c\bar{s}\mu\bar{\nu}_\mu\nu_e\bar{e}$. In other cases they can form two charged and two neutral couples (2Z2W), e.g., $u\bar{u} \to b\bar{b}\mu\bar{\nu}_\mu\nu_e\bar{e}$. In all other cases the full set of diagrams splits into a sum of the three basic gauge invariant sets mentioned above, and can be described as 2Z2W + 4Z, 4W + 2Z2W or 4W + 2Z2W + 4Z, e.g., $u\bar{d} \to u\bar{d}e\bar{\nu}_e\nu_e\bar{e}$. Similarly, all reactions with two external gluons and six fermions can be computed from two basic amplitudes which, with obvious notation, we call 2g2WZ and 2g3Z. From the above discussion it becomes clear why in PHANTOM we have eight master amplitudes: three pure electroweak with eight external fermions (4Z, 4W, 2Z2W) at $\mathcal{O}(\alpha_{EM}^6)$, the same three at $\mathcal{O}(\alpha_{EM}^6) + \mathcal{O}(\alpha_{EM}^4\alpha_S^2)$ and the two with two external gluons (2g2WZ and 2g3Z). We take moreover advantage of the fact that the diagrams in which two or more of the external particles are identical can be split in sets which just differ for the exchange of the identical particles. Therefore the master amplitude corresponds to the basic diagrams that one would have if all external particles were different. In PHANTOM the full amplitude of the process at hand is then computed by the routines `ampem.f`, `amp8fqcd.f`, `amp2g.f` which call all the necessary master amplitudes with the appropriate order of the momenta and call `coleval.f` or `colevalew.f` to evaluate the color factors. The amplitude routines compute separately the sum of the diagrammatic contributions for every possible color configuration. The probability used for choosing the color flow of each event, as specified by the Les Houches Accord File Format, is taken to be proportional to the modulus square of the amplitude of each configuration.

The range of reactions which are available in PHANTOM is substantially larger than in PHASE. All $\mathcal{O}(\alpha_{EM}^4\alpha_S^2)$ contributions with one virtual or two external gluons and the 4Z amplitude were not previously available, only two master amplitudes were needed and general routines to compose the different amplitudes and evaluate the color factors were not necessary.

3.3. Master amplitudes computation

In this section we want to show briefly how the computation of master amplitudes is organized. We will first consider a master amplitude for eight external fermions at $\mathcal{O}(\alpha_{EM}^4\alpha_S^2)$, with one gluon exchange and then the one for 2g2WZ. We refer to Ref. [19] for a description of the kind of strategy we use for $\mathcal{O}(\alpha_{EM}^6)$ eight-fermion master amplitudes.

In the first case the possible ways in which the gluon can be exchanged are depicted in Fig. 5.

This immediately shows that it is convenient to perform the calculation via the subprocesses of Fig. 6. Starting from the left, the first two correspond to the decay of a virtual boson or gluon to four fermions, the third and the fourth are building blocks in which two external fermions annihilate in a virtual boson or gluon which is inserted in the middle of a fermion line. At least one of the two ends of the fermion line does not correspond to an external particle. The other parts of the fermion line and its attachments can be easily combined with such building blocks in the method we use [20,21].

For the master amplitude of 2g2WZ we notice first of all that the possible electroweak configurations are those of Fig. 7. To obtain all possible diagrams of the master amplitude it is sufficient to attach in all possible ways the two external gluons.

This leads to the twelve color structures of Fig. 8 where the first two starting from left correspond to both gluons attached to the same quark line in all possible ways and the second two to the two gluons attached to two different quark lines. It is superfluous to remind that the configuration with the two external gluons forming a triple vertex with a gluon propagator attached to the quark line can always be reduced to a linear combination of configurations (a) and (b).

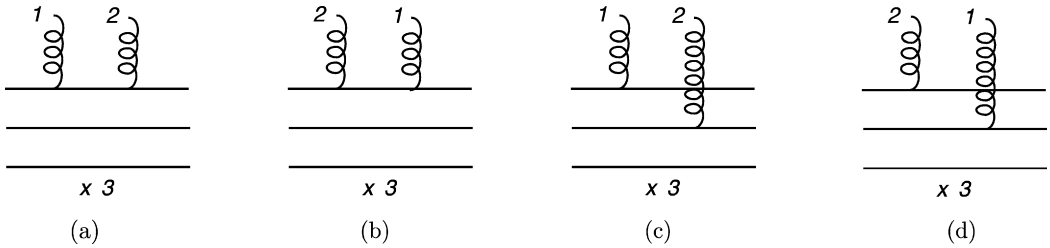

Fig. 8. Color structures of 2g2WZ.

Also for 2g2WZ we proceed evaluating subprocesses in order to avoid computing twice a subdiagram appearing in several different Feynman diagrams. Therefore one starts with subdiagrams of increasing complexity: virtual boson decaying to two fermions, to two fermions and one gluon and to two fermions and two gluons. Then those corresponding to one virtual fermion decaying to three fermions or three fermions and one gluon, etc. Putting together all these pieces one finally arrives at computing all groups of Feynman diagrams belonging to the same color structure, which is precisely the purpose of the routines computing the master amplitudes.

3.4. Parameters and parton distribution functions

Standard Model parameters are defined in the routine `coupling.f`. In our notation, `rmw`, `rmz`, `rmt`, and `rmb` are the W, Z, top and bottom masses respectively. The total W and Z widths are given by `gamw` and `gamz`. Higgs and top widths are computed in the same routine by standard formulas.

PHANTOM employs the G_μ-scheme defined by the input set: M_W, M_Z and G_F. According to this scheme, the calculated parameters are

$$\sin^2\theta_W = 1 - (M_W/M_Z)^2, \qquad \alpha_{em}(M_W) = \frac{\sqrt{2}}{\pi} G_F M_W^2 \sin^2\theta_W,$$

where θ_W is the weak mixing angle, and α_{em} the electromagnetic fine structure constant.

We introduce the decay width in the propagators of unstable particles using the fixed-width scheme. For the vector boson propagators, in the unitary gauge we work in, it consists in replacing M^2 with $M^2 - iM\Gamma$ both in the denominator and in the $p^\mu p^\nu$ term. This scheme preserves U(1) gauge invariance at the price of introducing unphysical widths for space-like vector bosons. A general discussion of the fixed-width scheme as well as of alternative approaches to introducing decay widths in scattering amplitudes can be found in the papers in Ref. [43].

For the PDF's we use the Les Houches Accord distribution [44], which can be downloaded from http://projects.hepforge.org/lhapdf/.

3.5. Iterative–adaptive multichannel

For completeness we describe in this section the iterative and adaptive multichannel technique which PHANTOM employs for integration. In our opinion the ability to adapt is the overriding consideration for multidimensional integrals of discontinuous and sharply peaked functions. An individual process can contain hundreds of diagrams and several unstable massive particles can appear at intermediate stages. The resonant peaking structure of the amplitude is therefore generally very rich. As a consequence the 16-dimensional phase space has multiple combinations of non-trivial kinematical regions corresponding to enhancements of the matrix element which need to be smoothed out in order to achieve a good convergence of the integration process, which in turn results in good efficiency of event generation.

We have merged the *multichannel* method [22] and the *adaptive* approach à la VEGAS [23]. An algorithm based on a similar philosophy has been proposed in [41]. In the *multichannel* approach, mappings into phase-space variables are chosen in such a way that the corresponding Jacobians cancel the peaks of the differential cross section. These mappings are not in general unique. One normally needs several different phase-space parametrizations, called channels, one for each possible peaking structure of the amplitude. This gives rise to a huge combinatorics which requires a correspondingly large number of channels. Number and type of these mappings must be fixed a priori, before starting the integration. The *multichannel* method thus requires a guess on the behavior of the integrand function. It indeed relies on the expectation that the selected set of channels, properly weighted [42], is able to describe reasonably well the amplitude. As no adaptivity is provided (apart from the freedom to vary the relative weight of the different channels), neglecting even one channel might worsen considerably the convergence of the integral.

The criteria of *adaptive* integration as performed by VEGAS are rather different. This approach bases its strength on the ability to deal automatically with totally unknown integrands. By employing an iterative method, it acquires knowledge about the integrand during integration, and adapts consequently its phase-space grid in order to concentrate the function evaluations in those regions where it peaks more. VEGAS divides the N-dimensional space in hypercubes, and scans the integrand along the axes. For a good convergence of the integral, it thus requires amplitude peaks to be aligned with the axes themselves. The problem can be easily solved if one set of phase-space variables is sufficient to describe the full amplitude peaking structure. In this case, the alignment can always be obtained by an appropriate variable transformation. The method becomes inefficient when it is impossible to align all enhancements with a single transformation.

In order to reduce the number of separate channels one has to consider in the *multichannel*, we use *multi-mapping*. In general multiple peaks can appear in the same variable, together with long non-resonant tails which extend far away from the peaks. This latter case is more and more severe as the collider energy increases. For instance the mass of a neutral fermion pair $f\bar{f}$ would typically resonate at both the Z and Higgs mass. The two peaks and the three non-resonant regions can be separately mapped into a five zone partition of the basic interval $[0, 1]$ of the integration variable. While *multi-mapping* is extremely useful to improve the convergence of VEGAS integration within a single phase-space parametrization, in general several such parametrizations are needed. In this case, one has to introduce N

different channels (in standard multichannel language) with their proper *multi-mapping*. Each channel defines a non-uniform probability density $g_i(\Phi)$, which describes a specific class of amplitude peaks. One can then write

$$I = \int d\Phi\, f(\Phi) = \sum_{i=1}^{N} \alpha_i \int \frac{d\Phi\, g_i(\Phi) f(\Phi)}{\sum_{i=1}^{N} \alpha_i g_i(\Phi)} = \sum_{i=1}^{N} \alpha_i \int dx_i\, f'\big(G_i^{-1}(x_i)\big) = \sum_{i=1}^{N} \alpha_i I_i \tag{1}$$

α_i being the so-called *weight* of the ith channel ($x_i = G_i(\Phi)$), and $f'(\Phi)$ the smoothed integrand. The α_i quantify the relevance of the different peaking structures of the amplitude. Owing to the very poor knowledge of the integrand, it is rather difficult to guess these values a priori. Usually, they are computed and optimized during the integration run. In the *iterative–adaptive multichannel*, the integral in Eq. (1) splits in N distinct contributions. The presence of identical final-state particles increases the possible list of resonant structures. In order to keep the number of separate integration runs manageable, we include all jacobians generated by particle exchange in the denominator of Eq. (1), while exploiting the freedom to relabel the momenta to regroup all integration runs related by particle exchange to a single one.

The integration proceeds through two steps: the first one which is called thermalization collects preliminary information about the integrand and fixes the weight of the different channels. In every thermalizing iteration, all channels are independently integrated for some set of α_i. At the end of each iteration, a new set of phase-space grids (one for each channel), and an improved set of α_i are computed. The criteria for weight optimization we adopt is

$$\alpha_i = \frac{I_i}{\sum_{i=1}^{N} I_i}, \tag{2}$$

where I_i is the i-channel integral. The new set of α_i and grids are then used in the next iteration. The procedure is repeated until a good stability of the α_i is reached. Weights smaller than 1×10^{-3} after the third thermalization iteration are set to zero and the corresponding channels are discarded. If any number of channels is dropped two additional thermalization iterations are performed. In the second step no further change of the weights is allowed, the total integral for each channel is evaluated and a corresponding phase space grid is produced. These grids are then stored and made available for event generation.

3.6. Phase space

While the number of possible combinations of resonances is very large, from a topological point of view the structure is much simpler. Apart from the weak vector bosons the only unstable particles in the SM which are relevant for LHC or ILC physics are the Higgs boson and the top quark. While the weak bosons at tree level have only two body decays, the top quark decays to bW and then to a three body system. For the Higgs boson the situation is more complex and the ratio of the various branching ratios and therefore their phenomenological relevance depends crucially on the Higgs mass. The Higgs decay channels however fall into two groups: two body decays like $\gamma\gamma$, $b\bar{b}$ or $\tau^+\tau^-$ or four body decays through W^+W^- or ZZ. It is therefore possible to construct a limited number of phase space parametrizations each of which, varying the masses and widths of the particles which appear in the intermediate states, can describe several channels in the multichannel sense.

In addition to s-channel resonances, t-channel enhancement can also be present. At the LHC they are regulated by minimum p_T requirements. At the ILC the issue is much more relevant because processes with electrons lost in the beam pipe can be an important background to charged current reactions.

Since we do not keep track of individual diagrams, the possible resonant structures must be deduced from the external particle content only. This is performed in the `proc.f` routine. Notice that the resonant structure depends on the perturbative order: $qq \to qqWW$ can have a $H \to WW$ resonance at $\mathcal{O}(\alpha_{EM}^6)$ but not at $\mathcal{O}(\alpha_{EM}^4 \alpha_S^2)$.

The criteria we adopt to automatically define number and type of channels needed for a given process are the following: for each process we consider all particles as outgoing and then examine all sets of four $f_i \bar{f}_j$ pairs which can be constructed, retaining only those in which all pairs can be identified with the decay products of a W or Z boson. This produces the complete set of possible two-particle enhancements. As a second step, for each selected set of pairs we search for triplets which reconstruct bW^+ and $\bar{b}W^-$ states and W^+W^- and ZZ states respectively. Pairs in which one fermion is outgoing and one incoming are associated with t-channel enhancements. For each set we determine the maximum number of enhancements which can be simultaneously present and introduce the corresponding channel in the list of channels utilized for the process. Multi-mapping and adaptivity will take care of all related partially-resonant or non-resonant configurations. Each channel in Eq. (1) is integrated separately with `VEGAS`.

In Fig. 9 we show pictorially the flexible phase space mappings which are available in `PHANTOM`. We denote by Ω_{ij} the usual angular variables in the center of mass of particles i and j and define $s_{i_1\ldots i_n} = (p_{i_1} + \cdots + p_{i_n})^2$ and $t_{ij} = (p_i - p_j)^2$. Then, for instance, the mapping corresponding to the central figure of the first row will use as variables t_{17}, t_{28}, s_{3456}, $\Omega_{(34)(56)}$, s_{34}, Ω_{34}, s_{56}, Ω_{56}, s_{34567}. The remaining variables are the azimuthal angles ϕ_8 and ϕ_7 of particle 8 in the overall center of mass and of particle 7 in the center of mass of 34567, respectively. If we indicate with M_X the invariant mass at which the s_X variable can resonate or the mass of the vector boson which enters into the t_X channel exchange, we could have $M_{17} = M_{28} = M_{34} = M_{56} = M_W$, $M_{3456} = M_H, M_Z$ which describes a WW fusion channel with a Higgs resonance; on the other hand we could also have $M_{17} = 0$, $M_{28} = M_{56} = M_W$, $M_{34} = M_Z$ which describes a $\gamma W \to ZW$ virtual scattering. It is clear that a large number of possible channels can be described by this single parametrization.

4. Running the program

4.1. Modes of operation

The program has two modes of operation which are selected by the input value `ionesh`. If `ionesh=0` the program computes the cross section for one single process, specified by `iproc`. If the input variable `iflat` is set to `1` the program produces one or more integration grids depending on the number of channels required for a good mapping of phase space for the selected process. If `ionesh=1` the

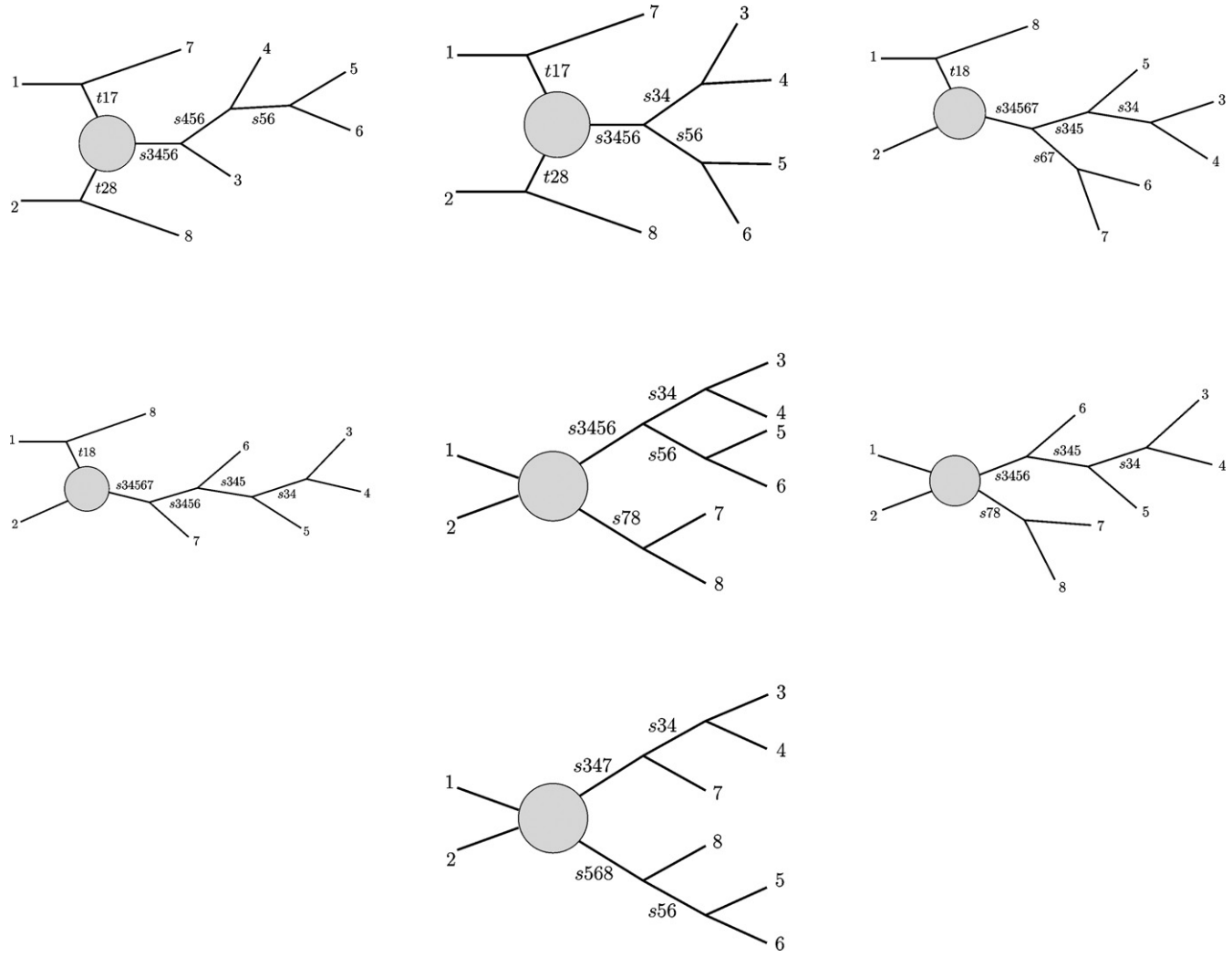

Fig. 9. Examples of phase space mappings.

program generates unweighted events for a set of processes, which is specified by the user, using the previously produced grids. All the integration grids for each selected process must be included for a meaningful generation.

When `ionesh=0` the program proceeds in two steps. The first one is called thermalization. It determines the relative weight of each channel in the multichannel integration and it produces a first instance of PHANTOM space grids, one per channel. At least three thermalization iterations are performed. At the end of the third iteration all channel whose relative weight is smaller than 10^{-3} are eliminated. If any channel is discarded, two additional thermalization iterations are performed, regardless of the flag `itmx_therm` mentioned below. The grids produced in the thermalization stage are then used as a starting point for the second step which consists of one integration per channel. Each integration will typically consist of several iterations and at each iteration the PHANTOM space grid will be refined in an effort to decrease the overall variance. A number of iterations between 3 and 5 is normally the best choice. If higher precision is requested it is usually more convenient to increase `ncall` rather than `itmx`. The user must be aware of the fact that if no point survives the cuts during an iteration, either during thermalization or at the integration stage, VEGAS will stop with an error.

At pp and e^+e^- colliders, when `ionesh=0` the process is computed exactly as specified by the user, assuming the first incoming particle to be moving in the $+z$ direction and the second one in the $-z$ direction. Even though at a pp collider this violates the symmetry between the two initial state protons, it can be useful for testing and for specialized studies. The full cross section can be easily obtained for unlike incoming partons by symmetrizing all distributions with respect to the beams and multiplying by a factor of two. At a $p\bar{p}$ collider the default for unlike incoming partons is to sum over the two possible assignement of the two partons to the beams. The behavior at pp colliders can, and typically should, be modified when `ionesh=1` by the flag `i_exchincoming`.

4.2. Input

The syntax of the input is almost identical to the one required by the CERN library routine FFREAD. Routines internal to PHANTOM are however used (`iread, rread`), so that real variables can (and must) be given in double precision.

All lines in the file of input must not exceed 80 characters, with the exception of filenames which can be 200 characters long. A * or C character at the beginning of a line identifies it as a comment line. Comment lines can be freely interspersed within the input file, with the only obvious exception that they must not interrupt a list of input values for a single array variable. The name of the variable to be read must be specified as the first word of a line (needs not to begin in column 1). Its value(s) must follow it. The list of values can span

several lines. Variables which are not needed for the process under study will be ignored. They can be left in the file without harm. All variables actually read from the input file will be reproduced in the output.

The input variable `iproc` specifies the desired process using the standard Monte Carlo particle numbering scheme:

d	u	s	c	b	e^-	ν_e	μ	ν_μ	τ	ν_τ	g
1	2	3	4	5	11	12	13	14	15	16	21

Antiparticles are coded with the opposite sign. The first two entries represent the initial state partons. Therefore the string

$$3 \quad -4 \quad 2 \quad -2 \quad 3 \quad -3 \quad 13 \quad -14 \tag{3}$$

corresponds to the reaction

$$s\bar{c} \to u\bar{u}s\bar{s}\mu\overline{\nu_\mu}. \tag{4}$$

4.3. Cuts

The program provides two means of specifying acceptance cuts. A basic predefined set can be imposed through the input file. They cover the usual requirement of minimum energy, transverse momentum and separation among the final state partons. All cuts are specified by an integer of the type `i_flag` which specifies whether the corresponding cut is activated (`i_flag=1`) or not (`i_flag=0`) and by one or more values which define the extrema of the accepted region. The name of the flag in most cases is the name of the corresponding variable with `i_` prepended.

The first part of the input cuts is common to both running modes, and must be always kept unchanged when passing from `ionesh=0` to `ionesh=1`. It constitutes in fact the setup under which phase-space grids are produced. In order to give the possibility of imposing other cuts at generation level, the *input-file* has also a cut section specific of the *one-shot* mode, The corresponding variables are the same as those in the common input section; they are just renamed with a suffix - `os` - appended. These additional cuts, operating at generation level, are obviously effective only if more restrictive than the common ones. Since no predefined set of cuts will be able to cover all possible user needs, it is also possible to include extra user-specified cuts via a routine called `iuserfunc`, an example of which is provided in the program package, inside the file `cuts.f` As for the predefined set of cuts, additional requirements can be imposed at generation level via the `iuserfuncos` routine. If user-specified cuts are imposed the package needs to be recompiled.

4.4. Output

The output of the program depends obviously on the mode of operation. The result of running the program in the integration phase (`ionesh=0`) is an output file in which are reported the input choices and the result of the various iterations during integration for the different channels. One can check from this file the accuracy reached by the integration and the reliability of the result. The informations needed for the successive unweighted event generations are given for channel *xx* of a given process by files under the name `phave-gasxx.dat`. For every process a separate directory must be created. The output of the (`ionesh=1`) mode is a file in which the statistics for each channel contributing to the generation are reported, as well as the total integral of all channels contributing to the generations. It is advisable to check that this result corresponds, within the statistical errors, to the sum of the cross sections of the various processes contributing to the final sample, taking into account possible factors of two due to the exchange of incoming particles. If one has set in input `iwrite_event 1`, as it is normally the case, the unweighted events generated at parton level are written in a file named `phamom.dat` using the Les Houches Accord File Format [45]. The way the events are written depends on the flag `iwrite_mothers`. If this is set to 1 additional information is added to the event concerning possible "mothers" (resonances) which generate final particles or intermediate "on shell" particles. This information is used by the hadronization Monte Carlo's and in particular by `PYTHIA` [46] for the evolution of the parton shower and the hadronization. Preliminary studies show that the use of this information has sizable consequences, at least for top processes, on the final fully hadronized events.[1] It is obvious that in a full calculation, the identification of the "mothers" in an event is not straightforward as it would be in a production times decay approximation. We have therefore chosen to somehow rely on the kinematic configuration of the event for assigning the "mothers". We first of all determine which are the possible mothers considering the particular phase space channel and parameters used to produce the kinematical configuration. We then look at the color configuration chosen via the amplitudes and test if the two informations agree. Only to those resonances which pass the check we assign the role of "mothers".

4.5. Scripts

Determining the minimal set of reactions for which grids need to be computed can be tedious and error prone. Therefore we have included in the distribution two Perl scripts `setupdir-all-LSF.pl` and `setupdir-all-LSF_ILC.pl` which handle the task for hadron and e^+e^- colliders respectively. The script can be executed with, for instance:

```
perl setupdir-all-LSF.pl [-options...]
```

where options include:

[1] We thank Roberto Chierici for pointing out this feature to us and Torbjorn Sjostrand and Fabio Maltoni for discussions on this point.

```
-basedir      directory which contains the exe file
              (full pathname)                          [./]
-dirtreeroot  root of new tree (full pathname)          [mh0]
-template     input template file                       [template.st0]
-executable   executable file                          [phantom.exe]
-inputstring  must contain only leptons and gluons     [""]
              must be enclosed in double quotes:
              "e e_ mu vm_"
              only processes containing -inputstring
              will be generated
-quarks       number of quarks to be inserted          [0]
              (even integer > 0 and <= 8)
-Top          number of intermediate top/antitop quarks which can
              be reconstructed by the final state particles
              (possible values 0,1,2). If the option is of the form
              n+ any reaction with at least n intermediate tops are
              accepted. If the option is not set any number of tops
              is accepted (equivalent to 0+).
-help         prints usage details
```

Long options can be abbreviated up to one letter, e.g. `-basedir X` can be passed as `-b X`. In square brackets the default values are reported. For each reaction the scripts create a directory which contains the corresponding `r.in` input file which is generated using the given template which must contain all input parameters with the exception of `iproc` which is supplied by the script. A runfile called `run` is also created. In the root directory of the new tree the script creates a file called `LSFfile` which can be used for submitting all integration jobs to the CERN LSF batch system. For different batch systems the user should appropriately edit the Perl scripts.

5. $\mathcal{O}(\alpha_{EM}^6) + \mathcal{O}(\alpha_{EM}^4\alpha_S^2)$ results in the semileptonic $\mu\nu_\mu$ channel

In this section we present an example of some phenomenological results obtained with PHANTOM. These studies have been performed via the generation of high statistic samples of unweighted events at parton level for all processes with a pair of leptons $\mu\bar{\nu}_\mu$ and different Higgs masses at the LHC. For a more complete discussion of other studies performed with PHANTOM we refer to [47].

We investigate how much the sensitivity to the VV scattering signal in the semileptonic $\mu\bar{\nu}_\mu$ channel is affected by the QCD irreducible background.

In the absence of firm predictions in the strong scattering regime, trying to gauge the possibilities of discovering signals of new physics at the LHC requires the somewhat arbitrary definition of a model of V_LV_L scattering beyond the boundaries of the SM. Some of these models predict the formation of spectacular resonances which will be easily detected. For some other set of parameters in the models only rather small effects are expected [48,49].

Two groups [50,51] have recently tried to parametrize the low energy behavior of large classes of composite Higgs models. They showed that the most characteristic signature is a reduced coupling between the Higgs state and the SM vector bosons, leading to only a partial cancellation of the growth of V_LV_L scattering amplitudes which would eventually result in violations of unitarity.

The predictions of SM in the presence of a very heavy Higgs provide an upper bound on the observability of such effects. The linear rise of the cross section with the invariant mass squared [52] in the hard VV scattering will be swamped by the decrease of the parton luminosities at large momentum fractions and, as a consequence, will be particularly challenging to detect.

In our study, we consider the full set of parton-level processes involved at $\mathcal{O}(\alpha_{EM}^6) + \mathcal{O}(\alpha_{EM}^4\alpha_S^2)$

$$qq \to qqqq\mu\bar{\nu}_\mu \qquad gg \to qqqq\mu\bar{\nu}_\mu$$
$$gq \to gqqq\mu\bar{\nu}_\mu \qquad qq \to ggqq\mu\bar{\nu}_\mu$$

together with a selection procedure as close as possible to the actual experimental practice, without resorting to any flavor information other than the one which a typical b-tagging algorithm is able to provide. A more complete analysis including the $4jW$ background at $\mathcal{O}(\alpha_{EM}^2\alpha_S^4)$ is left for a forthcoming paper.

The p_z of the neutrino is approximately reconstructed requiring the invariant mass of the two leptons to be equal to the W boson nominal mass. Its transverse momentum is assumed to be equal to the missing p_T.

All the results presented in this section have been obtained using the CTEQ5L PDF [53] set. The QCD coupling constant has been evaluated at the scale

$$Q^2 = M_{\text{top}}^2 + p_T(\text{top})^2, \tag{5}$$

where $p_T(\text{top})$ is the transverse momentum of the reconstructed top, for all processes in which a t or $\bar{t}$ can be produced. For all other processes the scale has been evaluated as

$$Q^2 = M_W^2 + \frac{1}{6}\sum_{i=1}^{6} p_{Ti}^2, \tag{6}$$

where p_{Ti} denotes the transverse momentum of the ith final state particle.

It should be clear from the results shown in Table 1 that suppressing the top background is the primary goal to achieve. In this analysis we assume the possibility to tag b-jets in the region $|\eta| < 1.5$ with 0.8 efficiency, which allows to discard part of the events containing

Table 1
Contribution of $t\bar{t}$/single t to the total cross section with standard acceptance cuts only (see the left part of Table 2). Comparison between results at $\mathcal{O}(\alpha_{EM}^6)$ (EW) and $\mathcal{O}(\alpha_{EM}^6)+\mathcal{O}(\alpha_{EM}^4\alpha_S^2)$ (EW + QCD). Interferences between the two perturbative orders are neglected.

$M_H = 200$ GeV	σ_{EW}	σ_{EW+QCD}
All events	0.89 pb	80.8 pb
Top events	0.52 pb	71.6 pb
Ratio top/all	0.58	0.89

Table 2
List of kinematical cuts applied in all results on the $\mu\nu_\mu$ channel.

Acceptance cuts	Selection cuts
$p_T(\ell^\pm, j) > 10$ GeV	b-tagging for $\|\eta\| < 1.5$ (80% efficiency)
$E(\ell^\pm, j) > 20$ GeV	$\|M(jjj; j\ell^\pm\nu_{\rm rec}) - M_{\rm top}\| > 15$ GeV
$\|\eta(\ell^\pm)\| < 3$	70 GeV $< M(j_c j_c) <$ 100 GeV
$\|\eta(j)\| < 6.5$	$M(j_f j_b) <$ 70 GeV; $M(j_f j_b) >$ 100 GeV
$M(jj) > 20$ GeV	$M(jj) > 60$ GeV
	$\Delta\eta(j_f j_b) > 4$
	$p_T(\ell^\pm\nu_{\rm rec}) > 100$ GeV
	$\eta(\ell^\pm\nu_{\rm rec}) < 2$
	$M(j_{f/b}\ell^\pm\nu_{\rm rec}) > 250$ GeV

j denotes any final-state quark or gluon, while $\ell^\pm$ is the charged lepton. The subfixes c, f, b mean *central*, *forward*, *backward* respectively. $\nu_{\rm rec}$ is the neutrino reconstructed following the prescription described in the text.

b quarks in the final state. We impose additional cuts against the top on the invariant mass of triplets of type $\{jjj\}$ and $\{j\mu\nu\}$, where j denotes any final-state quark or gluon. In order to isolate two vector boson production, kinematical cuts are applied on the invariant mass of the two most central jets, which are associated in our analysis to a W or Z decaying hadronically. The VV fusion signature is further isolated by requiring a minimum $\Delta\eta$ separation between the two forward/backward jets.

At this stage, however, any attempt to appreciate differences between Higgs and no-Higgs scenarios at high invariant masses would still be vain. This is essentially due to the fact that the contribution of the QCD diagrams is not substantially affected by the above-mentioned selection criteria. Investigating the differences between the kinematics of VV scattering and VV + 2 jets, we have identified additional cuts that serve our purpose. As the background dominates in the phase space regions characterized by vector boson emitted by the tag jets, a viable method of taming VV + 2 jets consists in applying cuts on the p_T and η of the W reconstructed from leptons as well as on the invariant mass of the W plus any of the two tag jets. All details about the selection cuts applied are reported in Table 2.

Fig. 10 illustrates the final results of our analysis, showing that the top background is basically under control. VV + 2 jets still provides a non-negligible contribution over the whole invariant mass spectrum, nevertheless differences between light-Higgs and no-Higgs can be appreciated.

In Tables 3, 4 we show the integrated cross section at high energies as a function of the minimum invariant mass, comparing results for the pure EW and the EW + QCD cases. Despite reducing the ratio between no-Higgs and light-Higgs cross sections, the inclusion of QCD background does not seem to compromise the possibility of detecting signals of EWSB at the LHC from an excess of scattering events. We find that about 500 events are expected above 800 GeV after one year of high luminosity running ($\mathcal{L} = 100$ fb^{-1}) in case of a Higgs boson with mass 200 GeV. The no-Higgs model predicts about 250 more events in accordance with the enhancement of the VV differential cross section at high energies. These numbers refer to the muon channel only and can obviously be improved by summing up the muon and electron channels. It should nevertheless be noticed that imposing a minimum ΔR separation among colored particles could degrade these preliminary results and requires further investigations.

6. Conclusions

We have described in detail the features of the Monte Carlo PHANTOM which is the first dedicated event generator for six fermion physics which can be used at high energy pp, $p\bar{p}$ and e^+e^- colliders. It has already been used for some phenomenological studies on boson–boson scattering physics at the LHC and a short example of its possibilities in this field has been presented. It will be used for further detailed analyses at parton level, which should also contribute to assess the complementary role of hadronic and e^+e^- colliders in this field. It is however important to stress that after partonic studies, more realistic ones with full event reconstruction and detector simulation are needed to fully exploit the physics possibilities. PHANTOM has been developed also as a tool for these more complete analyses.

The program can be downloaded from http://www.ph.unito.it/~ballestr/phantom where all new versions will be made available.

Acknowledgements

A.B. wishes to thank the Department of Theoretical Physics of Torino University for support.

This work has been supported by MIUR under contract 2006020509_004 and by the European Community's Marie-Curie Research Training Network under contract MRTN-CT-2006-035505 'Tools and Precision Calculations for Physics Discoveries at Colliders'.

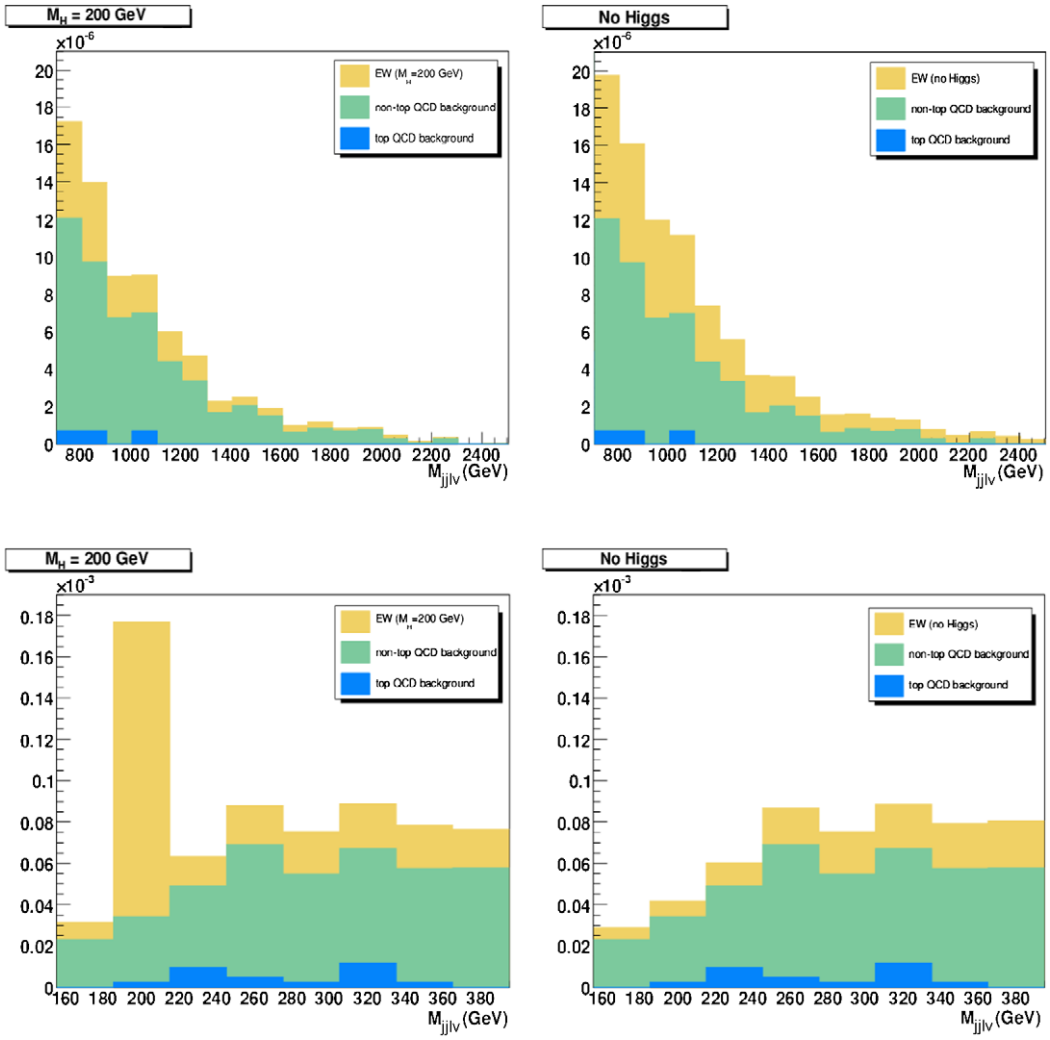

Fig. 10. Invariant mass distribution of the two leptons and the two most central jets in the Standard Model with a light Higgs (on the left) and in the no-Higgs scenario (on the right). The cuts applied are listed in Table 2. $\mathcal{O}(\alpha_{EM}^6)$ (EW) and $\mathcal{O}(\alpha_{EM}^4\alpha_S^2)$ (QCD) contributions to the differential cross section have been isolated and are shown separately. The QCD contributions are further split into *top background* (in blue) and VV + 2 jets (in green). (For interpretation of the references to color in this figure legend, the reader is referred to the web version of this article.)

Table 3
Integrated $\mathcal{O}(\alpha_{EM}^6)$ cross section for $M(j_c j_c l\nu) > M_{\text{cut}}$ and number of expected events after one year at high luminosity having applied the cuts listed in Table 2.

$\mathcal{O}(\alpha_{EM}^6)$	no Higgs		$M_H = 200$ GeV		Ratio
	σ (fb)	$\mathcal{L} = 100$ fb^{-1}	σ (fb)	$\mathcal{L} = 100$ fb^{-1}	
All events	12.46	1246 ± 35	13.57	1357 ± 37	0.918
$M_{\text{cut}} = 0.8$ TeV	3.19	319 ± 18	1.45	145 ± 12	2.200
$M_{\text{cut}} = 1.2$ TeV	1.28	128 ± 11	0.41	41 ± 6	3.122
$M_{\text{cut}} = 1.6$ TeV	0.60	60 ± 8	0.14	14 ± 4	4.286

Table 4
Integrated $\mathcal{O}(\alpha_{EM}^6) + \mathcal{O}(\alpha_{EM}^4\alpha_S^2)$ cross section for $M(j_c j_c l\nu) > M_{\text{cut}}$ and number of expected events after one year at high luminosity having applied the cuts listed in Table 2. Interferences between the two perturbative orders are neglected.

$\mathcal{O}(\alpha_{EM}^6) + \mathcal{O}(\alpha_{EM}^4\alpha_S^2)$	no Higgs		$M_H = 200$ GeV		Ratio
	σ (fb)	$\mathcal{L} = 100$ fb^{-1}	σ (fb)	$\mathcal{L} = 100$ fb^{-1}	
All events	40.70	4070 ± 64	40.73	4073 ± 64	0.999
$M_{\text{cut}} = 0.8$ TeV	7.61	761 ± 28	5.14	514 ± 23	1.481
$M_{\text{cut}} = 1.2$ TeV	2.53	253 ± 16	1.73	173 ± 13	1.462
$M_{\text{cut}} = 1.6$ TeV	1.00	100 ± 10	0.55	55 ± 7	1.818

Appendix A. Routines

Steering routines. The first one is the main program, the second drives the integration. The third, in generation mode, reads all grid files and steers the unweighted sampling.

```
phantom.f   integ.f   oneshot.f
```

Routine which parses the input file.

```
readinput.f
```

As the name indicates `coupling.f` computes the EW couplings in the G_μ-scheme, set masses and computes decay widths.

```
coupling.f
```

Modified `VEGAS` package.

```
phavegas.f
```

Integration function for `phavegas.f`

```
fxn.f
```

These routines select the set of channels to be used for each process and initialize the corresponding parameters.

```
proc.f   procini.f   procextraini.f
```

Phase space routines. The `XYZ_jac.f` routines, not shown here, compute the jacobian for the corresponding channel from the momenta.

```
phsp1_1_31_multi_c.f     phsp1_1_4_multi5_c.f
phsp1_2_3_multi5_c.f     phsp1_5to1_4to31_multi_c.f
phsp2_4_multi5.f         phsp2_4to31_multi5.f
phsp3_3_multi5.f
```

Beamstrahlung [54] and Initial State Radiation routines for e^+e^- colliders.

```
circe.f     isr.f
```

Implementing the cuts

```
cuts.f
```

These routines compute the complete amplitude for each process using the master amplitudes and the color evaluation routines mentioned below.

```
ampem.f   amp8fqcd.f   amp2g.f
```

Master amplitudes: 4W, 4Z, 2W2Z, 2g3Z, ggW2Z.

```
fourw.f      fourz.f      twoztwow.f
fourwqcd.f   fourzqcd.f   twoztwowqcd.f
gg3z.f       ggzww.f
```

Color evaluation routines

```
colevalew.f   coleval.f
```

Storing the event information according to the latest Les Houches Accord

```
LHAFileInit.f   storeLH.f
```

Utility routines

```
phread.f    bernoul.f   util.f     ccfcsym.f
extrema.f   isign.f     perm2g.f   perm.f
```

Appendix B. Sample input file

We report here a sample input file to integrate the process $\bar{b}\bar{b} \to \bar{b}\bar{b}\,\mu^+\mu^-\,\nu_\mu\,\bar{\nu}_\mu$. The lines starting with * and the text following a ! are comments which can be left without problem in the input file. One can use this same file to generate an unweighted sample with the same cuts and options, just changing `ionesh 0` in `ionesh 1` and fixing at the end the exact number of files `nfiles` and their names for the processes to be generated. The line containing the indication of the process (`iproc`) will in this case be ignored. It is evident

from the comments that some parts of the input are ignored when `ionesh=0` and some others when `ionesh=1`. We also recall that our convention is that whenever there is a `yes/no` option 1 corresponds to yes and 0 to no. The `EVENTUAL MORE RESTRICTIVE CUTS` are not all reported for brevity.

```
iproc    -5 -5 -5 -5 13 -13 14 -14

idum  -123456789   !random number seed must be a large negative number

PDFname   /home/phantom/phantom/lhapdf-5.2.2/PDFsets/cteq5l.LHgrid

*  i_PDFscale selects the PDF scale:
       ! =1 for all processes, based on pT's of ALL OUTGOING PARTICLES
       ! =2 process by process, based on pT of the (RECONSTRUCTED) TOP
       !    if possible, otherwise as done in option 1
i_PDFscale  2

*   i_coll  determines the type of accelerator:
*    1 => p-p   2 => p-pbar   3 => e+e-
i_coll  1

i_isr   0         ! yes/no ISR for e+e- collider only

i_beamstrahlung   0     ! yes/no beamstrahlung for e+e- collider only

* perturbativeorder = 1 alpha_em^6 with dedicated amp
*    2 alpha_s^2alpha_em^4   3 alpha_em^6 + alpha_s^2alpha_em^4
perturbativeorder 3

ionesh  0   ! 0= one process run, 1= one shot generation

ecoll    14000.d0    ! collider energy

rmh      -500.d0   ! Higgs mass (GeV). If negative Higgs diagrams are not
                   ! computed: equivalent to rmh=infinity.

i_ccfam  1           ! yes/no family+CC conjugate

* CUTS

i_e_min_lep    1         ! yes/no lepton energy lower cuts (GeV)
e_min_lep      20.d0

i_pt_min_lep   1       ! yes/no lepton pt lower cuts (GeV)
pt_min_lep     10.d0

i_eta_max_onelep 0   ! yes/no at least one lepton in absval of
                     ! eta_max_onelep. If no leptons are present
                     ! in the final state cut is ignored
eta_max_onelep    3.d0

i_eta_max_lep  1       ! yes/no lepton rapidity upper cuts
eta_max_lep    3.d0

i_ptmiss_min  0        ! yes/no missing pt lower cuts
ptmiss_min    50.d0

i_e_min_j     1        ! yes/no jet energy lower cuts (GeV)
e_min_j       20.d0

i_pt_min_j    1       ! yes/no jet pt lower cuts (GeV)
pt_min_j      10.d0

i_eta_max_j   1       ! yes/no jet rapidity upper cuts
eta_max_j     6.5d0

i_eta_jf_jb_jc   0    ! yes/no the following 3 cuts
```

```
eta_def_jf_min 1.d0   ! min rapidity for a jet to be called forward
eta_def_jb_max -1.d0  ! max rapidity for a jet to be called backward
eta_def_jc_max 3.d0   ! max rapidity for a jet to be called central
                      !       (absval)

i_pt_min_jcjc 0       ! pt lower cut on two centraljets (GeV)
pt_min_jcjc 50.d0

i_rm_min_jj 1      ! yes/no minimum invariant mass  between jets (GeV)
rm_min_jj 20.d0

i_rm_min_ll 1     ! yes/no minimum invariant mass between charged lept.
rm_min_ll 20.d0

i_rm_min_jlep 0  ! yes/no minimum invariant mass between jets and lepton
rm_min_jlep 30.d0

i_rm_min_jcjc 0     ! yes/no minimum invariant mass between central jets
rm_min_jcjc 20.d0

i_rm_max_jcjc 0     ! yes/no maximum invariant mass between central jets
rm_max_jcjc 14000.d0

i_rm_min_jfjb  0   ! yes/no minimum invariant mass between forward
                   !and backward jets
rm_min_jfjb 100.d0

i_eta_min_jfjb 0  ! yes/no minimum rapidity difference between forward
                  ! and backward jet
eta_min_jfjb 3.d0

i_d_ar_jj 0  ! yes/no minimum delta_R separation  between jets
d_ar_jj 0.7d0

i_d_ar_jlep 0  !yes/no minimum delta_R separation between jets and lepton
d_ar_jlep 0.7d0

i_thetamin_jj 0  ! yes/no minimum angle separation between jets (degrees)
thetamin_jj    15.d0

i_thetamin_jlep 0  ! yes/no minimum angle separation between jets
                   ! and lepton (degrees)
thetamin_jlep    15.d0

i_thetamin_leplep 0 ! yes/no minimum angle separation between charged
                    ! leptons (cosine)
thetamin_leplep    15.d0

i_usercuts 0    ! yes/no (1/0) additional   user-defined cuts


****** IF (IONESH.EQ.0) THEN

acc_therm     0.01d0      ! thermalization accuracy

ncall_therm   300000  3000000     ! thermalization calls per iteration
                    ! for the first 3 and for the remaining iterations
itmx_therm    5                   ! thermalization iterations

acc           0.005d0         ! integration accuracy

ncall         5000000           ! integration calls per iteration

itmx          5             ! integration iterations

iflat         1         ! yes/no flat event generation
```

```
****** ELSEIF (IONESH.EQ.1) THEN

scalemax  1.1d0             !scale factor for the maximum

nunwevts   20000     !  number of unweighted events to be produced

iwrite_event 1   ! yes/no momenta of flat events written in.dat files

iwrite_mothers 1   ! yes/no information about intermediate
                   !  particles (mothers) in.dat files

i_exchincoming  1

*           EVENTUAL MORE RESTRICTIVE CUTS:
*           SAME LIST AS BEFORE WITH "os" POSTPENDED

iextracuts  0  ! yes/no more restrictive cuts at generation level

i_e_min_lepos  0             ! lepton energy lower cuts (GeV)
e_min_lepos    30.d0
.
.
.
i_usercutsos  0

*  nfiles= number of files from which take the input for
*          oneshot generation
nfiles   3    ! number of input files for oneshot generation
/home/phantom/phantom/process1/phavegas01.dat
/home/phantom/phantom/process1/phavegas02.dat
/home/phantom/phantom/process2/phavegas01.dat
```

References

[1] M.L. Mangano, M. Moretti, F. Piccinini, R. Pittau, A.D. Polosa, JHEP 0307 (2003) 001, hep-ph/0206293.
[2] F. Maltoni, T. Stelzer, JHEP 0302 (2003) 027;
T. Stelzer, W.F. Long, Comput. Phys. Comm. 81 (1994) 357;
J. Alwall, et al., arXiv: 0706.2334;
H. Murayama, I. Watanabe, K. Hagiwara, KEK-91-11.
[3] E. Accomando, A. Ballestrero, S. Bolognesi, E. Maina, C. Mariotti, JHEP 0603 (2006) 093, hep-ph/0512219.
[4] M.S. Chanowitz, M.K. Gaillard, Nucl. Phys. B 261 (1985) 379;
M.S. Chanowitz, M.K. Gaillard, Phys. Lett. B 142 (1984) 85 and Ref. [1];
G. Kane, W. Repko, B. Rolnick, Phys. Lett. B 148 (1984) 367;
S. Dawson, Nucl. Phys. B 249 (1985) 42.
[5] E. Accomando, A. Ballestrero, A. Belhouari, E. Maina, Phys. Rev. D 74 (2006) 073010, hep-ph/0608019.
[6] S.R. Slabospitsky, L. Sonnenschein, Comp. Phys. Comm. 148 (2002) 87, hep-ph/0201292.
[7] S. Tsuno, T. Kaneko, Y. Kurihara, S. Odaka, K. Kato, Comput. Phys. Comm. 175 (2006) 665, hep-ph/0602213.
[8] S. Dittmaier, M. Roth, Nucl. Phys. B 642 (2002) 307, hep-ph/0206070.
[9] G. Montagna, et al., Eur. Phys. J. C 2 (1998) 483;
F. Gangemi, et al., Eur. Phys. J. C 9 (1999) 31; Nucl. Phys. B 559 (1999) 3.
[10] E. Accomando, et al., Nucl. Phys. B 512 (1998) 19; Nucl. Phys. B 547 (1999) 81.
[11] K. Kolodziej, Comput. Phys. Comm. 151 (2003) 339.
[12] S. Moretti, Phys. Lett. B 420 (1998) 367; Nucl. Phys. B 544 (1999) 289.
[13] F. Krauss, R. Kühn, G. Soff, JHEP 0202 (2002) 044;
A. Schalicke, F. Krauss, R. Kühn, G. Soff, JHEP 0212 (2002) 013.
[14] E.E. Boos, M.N. Dubinin, V.A. Ilyin, A.E. Pukhov, V.I. Savrin, hep-ph/9503280;
A. Pukhov, et al., hep-ph/9908288.
[15] T. Ishikawa, et al., Minami-Tateya Collaboration, KEK-92-19;
H. Tanaka, et al., Minami-Tateya Collaboration, Nucl. Instrum. Meth. A 389 (1997) 295;
F. Yuasa, et al., Prog. Theor. Phys. 138 (Suppl.) (2000) 18;
S. Tsuno, K. Sato, J. Fujimoto, T. Ishikawa, Y. Kurihara, S. Odaka, T. Abe, Comput. Phys. Comm. 151 (2003) 216.
[16] C.G. Papadopoulos, Comput. Phys. Comm. 137 (2001) 247;
A. Kanaki, C.G. Papadopoulos, Comput. Phys. Comm. 132 (2000) 306;
A. Cafarella, C.G. Papadopoulos, M. Worek, arXiv: 0710.2427 [hep-ph].
[17] M. Moretti, T. Ohl, J. Reuter, hep-ph/0102195;
W. Kilian, LC-TOOL-2001-039, Jan 2001, in: 2nd ECFA/DESY Study 1998-2001, 1924–1980;
W. Kilian, T. Ohl, J. Reuter, arXiv: 0708.4233 [hep-ph].
[18] T. Gleisberg, F. Krauss, C.G. Papadopoulos, A. Schaelicke, S. Schumann, Eur. Phys. J. C 34 (2004) 173, hep-ph/0311273.
[19] E. Accomando, A. Ballestrero, E. Maina, JHEP 0507 (2005) 016, hep-ph/0504009.
[20] A. Ballestrero, E. Maina, Phys. Lett. B 350 (1995) 225, hep-ph/9403244.
[21] A. Ballestrero, PHACT 1.0—Program for helicity amplitudes calculations with Tau matrices, in: B.B. Levchenko, V.I. Savrin (Eds.), Proceedings of the 14th International Workshop on High Energy Physics and Quantum Field Theory (QFTHEP 99), SINP MSU, Moscow, p. 303, hep-ph/9911318.

[22] F.A. Berends, R. Pittau, R. Kleiss, Nucl. Phys. B 424 (1994) 308; Comput. Phys. Comm. 85 (1995) 437;
F.A. Berends, P.H. Daverveldt, R. Kleiss, Nucl. Phys. B 253 (1985) 441;
J. Hilgart, R. Kleiss, F. Le Diberder, Comput. Phys. Comm. 75 (1993) 191.
[23] G.P. Lepage, J. Comp. Phys. 27 (1978) 192.
[24] E. Accomando, A. Ballestrero, E. Maina, Comput. Phys. Comm. 150 (2003) 166;
E. Accomando, A. Ballestrero, Comput. Phys. Comm. 99 (1997) 270.
[25] ATLAS Collaboration, Detector and Physics Performance Technical Design Report, vols. 1 and 2, CERN-LHCC-99-14 and CERN-LHCC-99-15.
[26] CMS Collaboration, CMS Physics Technical Design Report, CERN/LHCC 2006–001.
[27] A. Djouadi, J. Lykken, K. Monig, Y. Okada, M.J. Oreglia, S. Yamashita, International Linear Collider Reference Design Report, vol. 2: PHYSICS AT THE ILC, arXiv: 0709.1893 [hep-ph].
[28] S. Asai, et al., Eur. Phys. J. C 32S2 (2004) s19–s54, hep-ph/0402254.
[29] S. Abdulin, et al., CMS Note 2003/033.
[30] K. Crammer, et al., hep-ph/0401148.
[31] G. Jarlskog, D. Rein (Eds.), Proceedings of the Large Hadron Collider Workshop, Aachen 1990, CERN Report 90–10.
[32] A. Djouadi, The anatomy of electro-weak Symmetry Breaking. Tome I: The Higgs in the Standard Model, hep-ph/0503172.
[33] K.A. Assamagan, M. Narain, A. Nikitenko, M. Spira, D. Zeppenfeld, et al., Report of the Higgs Working Group, in: Les Houches 2003, Physics at TeV colliders, pp. 1–169, hep-ph/0406152.
[34] M.S. Chanowitz, Strong WW scattering at the end of the 90's: theory and experimental prospects, in: Zuoz 1998, Hidden Symmetries and Higgs Phenomena, pp. 81–109 hep-ph/9812215.
[35] M.J. Duncan, G.L. Kane, W.W. Repko, Nucl. Phys. B 272 (1986) 517;
D.A. Dicus, R. Vega, Phys. Rev. Lett. 57 (1986) 1110;
J.F. Gunion, J. Kalinowski, A. Tofighi-Niaki, Phys. Rev. Lett. 57 (1986) 2351.
[36] R.N. Cahn, S.D. Ellis, R. Kleiss, W.J. Stirling, Phys. Rev. D 35 (1987) 1626;
V. Barger, T. Han, R. Phillips, Phys. Rev. D 37 (1988) 2005; Phys. Rev. D 36 (1987) 295;
R. Kleiss, J. Stirling, Phys. Lett. B 200 (1988) 193;
V. Barger, et al., Phys. Rev. D 42 (1990) 3052;
V. Barger, et al., Phys. Rev. D 44 (1991) 1426;
V. Barger, et al., Phys. Rev. D 46 (1992) 2028;
D. Froideveaux, in Ref. [31], vol. II, p. 444;
M.H. Seymour, ibid., p. 557;
U. Baur, E.W.N. Glover, Phys. Lett. B 252 (1990) 683;
D. Dicus, J. Gunion, R. Vega, Phys. Lett. B 258 (1991) 475;
D. Dicus, J. Gunion, L. Orr, R. Vega, Nucl. Phys. B 377 (1992) 31;
U. Baur, E.W.N. Glover, Nucl. Phys. B 347 (1990) 12.
[37] J. Bagger, et al., Phys. Rev. D 49 (1994) 1246;
V. Barger, R. Phillips, D. Zeppenfeld, Phys. Lett. B 346 (1995) 106;
J. Bagger, et al., Phys. Rev. D 52 (1995) 3878;
K. Iordanidis, D. Zeppenfeld, Phys. Rev. D 57 (1998) 3072.
[38] D. Rainwater, D. Zeppenfeld, Phys. Rev. D 60 (1999) 113004; Erratum, Phys. Rev. D 61 (2000) 099901;
D. Rainwater, hep-ph/9908378.
[39] B. Jäger, C. Oleari, D. Zeppenfeld, JHEP 0607 (2006) 015, hep-ph/0603177;
B. Jäger, C. Oleari, D. Zeppenfeld, Phys. Rev. D 73 (2006) 113006, hep-ph/0604200;
G. Bozzi, B. Jäger, C. Oleari, D. Zeppenfeld, Phys. Rev. D 75 (2007) 073004, hep-ph/0701105.
[40] T. Binoth, G. Ossola, C.G. Papadopoulos, R. Pittau, JHEP 0806 (2008) 082, arXiv: 0804.0350 [hep-ph].
[41] T. Ohl, Comput. Phys. Comm. 120 (1999) 13.
[42] R. Kleiss, R. Pittau, Comput. Phys. Comm. 83 (1994) 141.
[43] E.N. Argyres, et al., Phys. Lett. B 358 (1995) 339;
W. Beenakker, et al., Nucl. Phys. B 500 (1997) 255;
U. Baur, D. Zeppenfeld, Phys. Rev. Lett. 75 (1995) 1002;
G. Passarino, Nucl. Phys. B 574 (2000) 451;
G. Passarino, Nucl. Phys. B 578 (2000) 3;
E. Accomando, A. Ballestrero, E. Maina, Phys. Lett. B 479 (2000) 209.
[44] http://projects.hepforge.org/lhapdf/.
[45] J. Alwall, et al., A Standard format for Les Houches event files. Written within the framework of the MC4LHC-06 workshop: Monte Carlos for the LHC: A Workshop on the Tools for LHC Event Simulation (MC4LHC), Geneva, Switzerland, 17–16 July 2005, Comput. Phys. Comm. 176 (2007) 300, hep-ph/0609017.
[46] T. Sjostrand, S. Mrenna, P. Skands, JHEP 0605 (2006) 026, hep-ph/0603175.
[47] E. Accomando, A. Ballestrero, A. Belhouari, E. Maina, Phys. Rev. D 75 (2007) 113006, hep-ph/0603167.
[48] J. Bagger, et al., Phys. Rev. D 52 (1995) 3878;
A. Dobado, M.J. Herrero, J.R. Peláez, E. Ruiz Morales, Phys. Rev. D 62 (2000) 055011, hep-ph/9912224.
[49] J.M. Butterworth, B.E. Cox, J.R. Forshaw, Phys. Rev. D 65 (2002) 096014, hep-ph/0201098.
[50] G.F. Giudice, C. Grojean, A. Pomarol, R. Rattazzi, hep-ph/0703164.
[51] R. Barbieri, B. Bellazzini, V.S. Rychkov, A. Varagnolo, arXiv: 0706.0432.
[52] S. Weinberg, Phys. Rev. Lett. 17 (1966) 616;
M.S. Chanowitz, M. Golden, H.M. Georgi, Phys. Rev. D 36 (1987) 1490; Phys. Rev. Lett. 57 (1986) 2344.
[53] H.L. Lai, et al., CTEQ Coll., Eur. Phys. J. C 12 (2000) 375.
[54] T. Ohl, Comput. Phys. Comm. 101 (1997) 269.